



PERGAMON

Available online at [www.sciencedirect.com](http://www.sciencedirect.com)

SCIENCE @ DIRECT®

Journal of Asian Earth Sciences xx (0000) xxx–xxx

Journal of Asian  
Earth Sciences[www.elsevier.com/locate/jseas](http://www.elsevier.com/locate/jseas)

# Fragments of oceanic islands in accretion–collision areas of Gorny Altai and Salair, southern Siberia, Russia: early stages of continental crustal growth of the Siberian continent in Vendian–Early Cambrian time

N.L. Dobretsov<sup>a</sup>, M.M. Buslov<sup>a,\*</sup>, Uchio Yu<sup>b</sup><sup>a</sup>United Institute of Geology, Geophysics, and Mineralogy, SB RAS, Novosibirsk 630090, Russian Federation<sup>b</sup>Department of Earth and Planetary Science, Graduate School of Engineering, Tokyo Institute of Technology, Tokyo, Japan

## Abstract

The Altai-Salair area in southern Siberia is a Caledonian folded area containing fragments of Vendian–Early Cambrian island arcs. In the Vendian–Early Cambrian, an extended system of island arcs existed near the Paleo-Asian Ocean/Siberian continent boundary and was located in an open ocean realm. In the present-day structural pattern of southern Siberia, the fragments of Vendian–Early Cambrian ophiolites, island arcs and paleo-oceanic islands occur in the accretion–collision zones. We recognized that the accretion–collision zones were mainly composed of the rock units, which were formed within an island-arc system or were incorporated in it during the subduction of the Paleo-Asian Ocean under the island arc or the Siberian continent. This system consists of accretionary wedge, fore-arc basin, primitive island arc and normal island arc. The accretionary wedges contain the oceanic island fragments consist of OIB basalts and siliceous–carbonate cover including top and slope facies sediments. Oceanic islands submerged into the subduction zone and, later were incorporated into an accretionary wedge. Collision of oceanic islands and island arcs in subduction zones resulted in reverse currents in the accretionary wedge and exhumation of high-pressure rocks. Our studies of the Gorny Altai and Salair accretionary wedges showed that the remnants of oceanic crust are mainly oceanic islands and ophiolites. Therefore, it is important to recognize paleo-islands in folded areas. The study of paleo- islands is important for understanding the evolution of accretionary wedges and exhumation of subducted high-pressure rocks.

© 2003 Published by Elsevier Science Ltd.

**Keywords:** Ophiolites; Paleo-oceanic; Fragments

## 1. Introduction

It is a common knowledge that fragments of paleo-oceanic lithosphere are preserved in foldbelts. In previous studies, various types of ophiolites have been commonly identified as oceanic crust fragments (Coleman, 1977; Dobretsov et al., 1977; Dobretsov and Zonenshain, 1985; Nicolas, 1989). During recent years, numerous fragments of oceanic islands and plateaus have been identified in foldbelts of different ages.

The general problem is that oceanic islands and basaltic plateaus in present oceans constitute significant volumes and areas in comparison with island arcs (Fig. 1). The elevation of oceanic islands and plateaus above the oceanic floor ranges from 1.5 to 5 km, the thickness of crust varies from 14 to 35 km, and the area varies from 100 km<sup>2</sup> for individual islands to 100,000 km<sup>2</sup> for oceanic plateaus, e.g.

Shatsky, Ontong-Java, Kergullen (Fig. 1). Therefore, we can expect that fragments of such structures should be widely present in foldbelts and their volume should be comparable with that of island arc fragments. The fact that they are less common in folded areas can be explained either by their subduction or by difficulties during their recognition among other sedimentary and basaltic-sedimentary terranes.

A possibility for preservation of the fragments of oceanic islands and oceanic plateaus was discussed in Ben-Avraham et al. (1981), Cloos (1993), Chekhovich (1997) and Bogdanov and Dobretsov (2002). After some simplification, we propose three scenarios for interaction of oceanic islands and subduction zones which are controlled by the thickness of oceanic crust and the height of oceanic rises.

1. If oceanic crust thickness is less than 14 km, and the height of oceanic rises is less than 2 km, most oceanic islands and plateaus would be completely subducted and only small fragments can be preserved in olistostromes. The examples of this scenario were

\* Corresponding author. Tel./fax: +7-3832-333584.

E-mail address: [misha@uiggm.nsc.ru](mailto:misha@uiggm.nsc.ru) (M.M. Buslov).

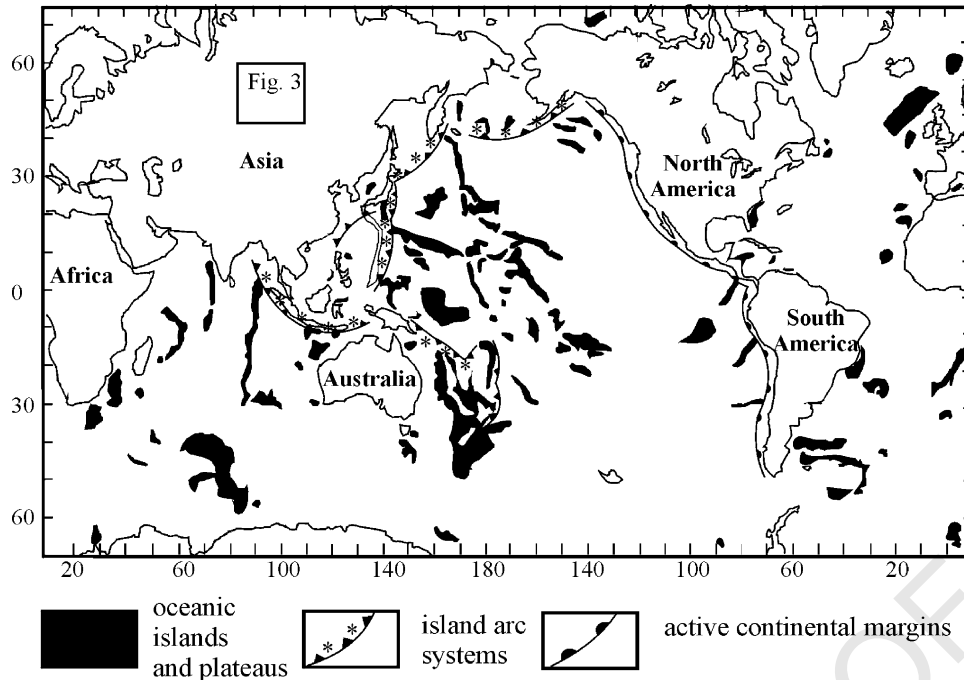


Fig. 1. The distribution of oceanic islands and islands in the world's oceanic basins (Nur and Ben-Avraham, 1982).

reported in Masson et al. (1990), Collot and Fisher (1991) and Von Huene and Scholl (1991) and others.

2. If oceanic crust thickness is 15–20 km, and the height of oceanic rises ranges from 2 to 4 km, larger fragments can be preserved, e.g. sedimentary or basaltic-sedimentary tops of islands, which were detached during subduction and incorporated into the subduction-accretionary complex.
3. If oceanic crust thickness is 20–30 km, and the height of rises is more than 4 km, oceanic islands could be accreted to an island arc or partly/completely 'swallowed' up by a subduction zone due to their negative buoyancy in response to their eclogitization and high-pressure metamorphism. The possibility of such transformations and velocity of exhumation depend on the age and velocity of subduction, total weight of an island and rheological properties of rocks. Eclogitization and exhumation processes were discussed in the models reported in Cloos (1993) and Dobretsov and Kirdyashkin (1992, 1998). The examples are the Akyoshi terrane in Japan (Kanmera and Sano, 1991), and several terranes in Gorny Altai and Salair as described in this paper.

The Carboniferous-Permian Akioshi terrane was one of the first examples of such units to be recognized (Kanmera and Sano, 1991). A thorough study of the Akioshi terrane showed the presence of shallow-water reef limestones on top of an oceanic island and slope sedimentary facies composed of carbonate-siliceous rocks of spiculites, underlain by deep-water foot-hill radiolarites and turbidite

siliceous and carbonate-siliceous silts, sandstones and siliceous tuffs bounding the slopes of the islands (Fig. 2).

There are several important aspects in paleogeographic reconstruction of oceanic islands whose fragments are incorporated into foldbelts. The first aspect implies the total absence of terrigenous materials in the rock of oceanic islands. The second point concerns lateral transition between massive limestone and the radiolarian chert succession through the detrital limestone succession containing spicular chert interbeds and a spicular chert succession containing lenses of redeposited limestone (Fig. 2).

Since the early 1990s many geoscientists have attempted to recognize oceanic terranes in the Altai-Sayan area (ASA). The Katun and Baratal terranes, probably the fragments of oceanic islands, were described in Buslov et al. (1993) and shown to the participants of the IGCP 283 post-symposium excursion. This paper presents new data obtained during the 1994–2000 field missions to Gorny Altai and Salair. These data support the previous recognition of oceanic island fragments and provide additional information on their composition, structure, age and relationships with surrounding olistostromes and high-pressure metamorphic rocks (Buslov and Watanabe, 1996; Buslov et al., 2001, 2002).

Gorny Altai and Salair are parts of Caledonian foldbelts in the southern frame of the Siberian craton. The fragments of ophiolites and oceanic islands once belonged to the Vendian–Early Cambrian crust of the Paleo-Asian Ocean (Dobretsov and Zonenshain, 1985; Zonenshain et al., 1990; Buslov et al., 1993; Berzin and Dobretsov, 1994; Dobretsov et al., 1995).

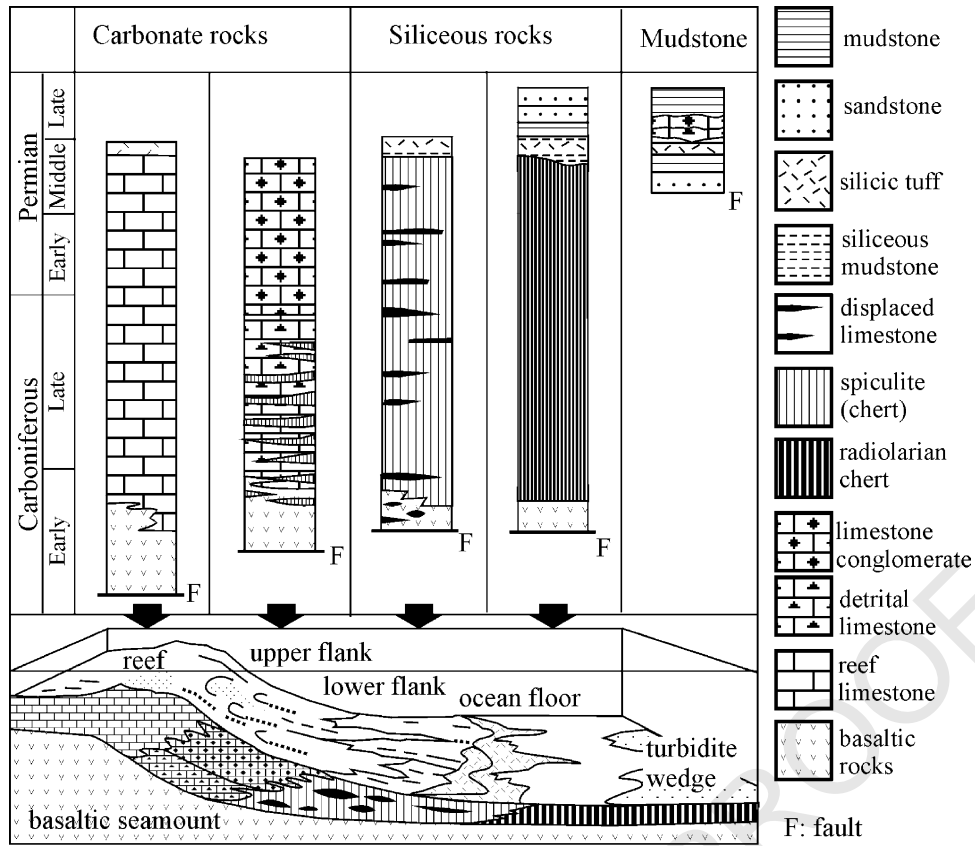


Fig. 2. Composite columnar sections summarizing the lithostratigraphy and age of Akiyoshi terrane rocks and the sedimentary-framework model for oceanic rocks (Kanmera and Sano, 1991).

## 2. Tectonic setting

Southern Siberia (Fig. 3) comprises a Caledonian folded area containing fragments of Vendian–Early Cambrian island arcs (Zonenshain et al., 1990; Sengor et al., 1993; Berzin and Dobretsov, 1994; Dobretsov et al., 1995; Buslov et al., 2001). In the Vendian–Early Cambrian, an extended system of island arcs existed between the Paleo-Asian Ocean and the Siberian continent. In the present-day structural pattern of southern Siberia and Mongolia (Fig. 3), the fragments of the Vendian–Early Cambrian ophiolites, island arcs and paleo-oceanic islands are incorporated into accretion–collision units which were faulted in the Late Paleozoic.

The accretion–collision zones consist of accretionary wedge, fore-arc basin, primitive and normal island arcs (Buslov and Watanabe, 1996; Buslov et al., 2001; Dobretsov et al., 1995). The oceanic islands submerged into the subduction zone and later were incorporated into an accretionary wedge. Concerning the exhumation of high-pressure rocks that also occur in the accretionary wedges, we suggest that collision of oceanic islands with an island arc generates reverse currents in the subduction zone (Dobretsov and Kirdyashkin, 1992, 1998) which cause the exhumation (blueschists, eclogites, etc.). In Southern Siberia, the fragments of paleo-oceanic islands

in the accretionary wedges are usually cemented by olistostromes containing fragments of the oceanic islands and island arc units. We infer that in response to the oceanic island–island arc collision, the subduction zones jumped oceanwards. Fore-arc basins overlying these complicated structures are filled with up to 6–8 km thick pelagic sediments and turbidites. The turbidites mainly consist of fragments and debris of island-arc and accretionary units.

Temporal and lateral compositional changes of magmatic rocks of island arcs in Southern Siberia are similar to modern volcanic arcs. Vendian and earliest Early Cambrian tholeiite–boninite series of the early stage reveal similarities to boninites in the Bonin Islands, Mariana and Tonga arcs. Tholeiite–calc-alkaline and, to a lesser degree, calc-alkaline normal arc volcanic series of the later stage, are similar to rocks of the mature Japan, Kuril, and Kamchatka volcanic arcs. Laterally, volcanic units within large fragments of normal island arcs range in composition from tholeiitic high-Mg andesite and basaltic rocks near fore-arc basins, through calc-alkaline rocks in the central parts to shoshonitic rocks in back-arc basins.

Vendian–Cambrian units in southern Siberia and Mongolia (Fig. 3) represent (1) Vendian–Early Cambrian oceanic islands formed above within-plate hot spots

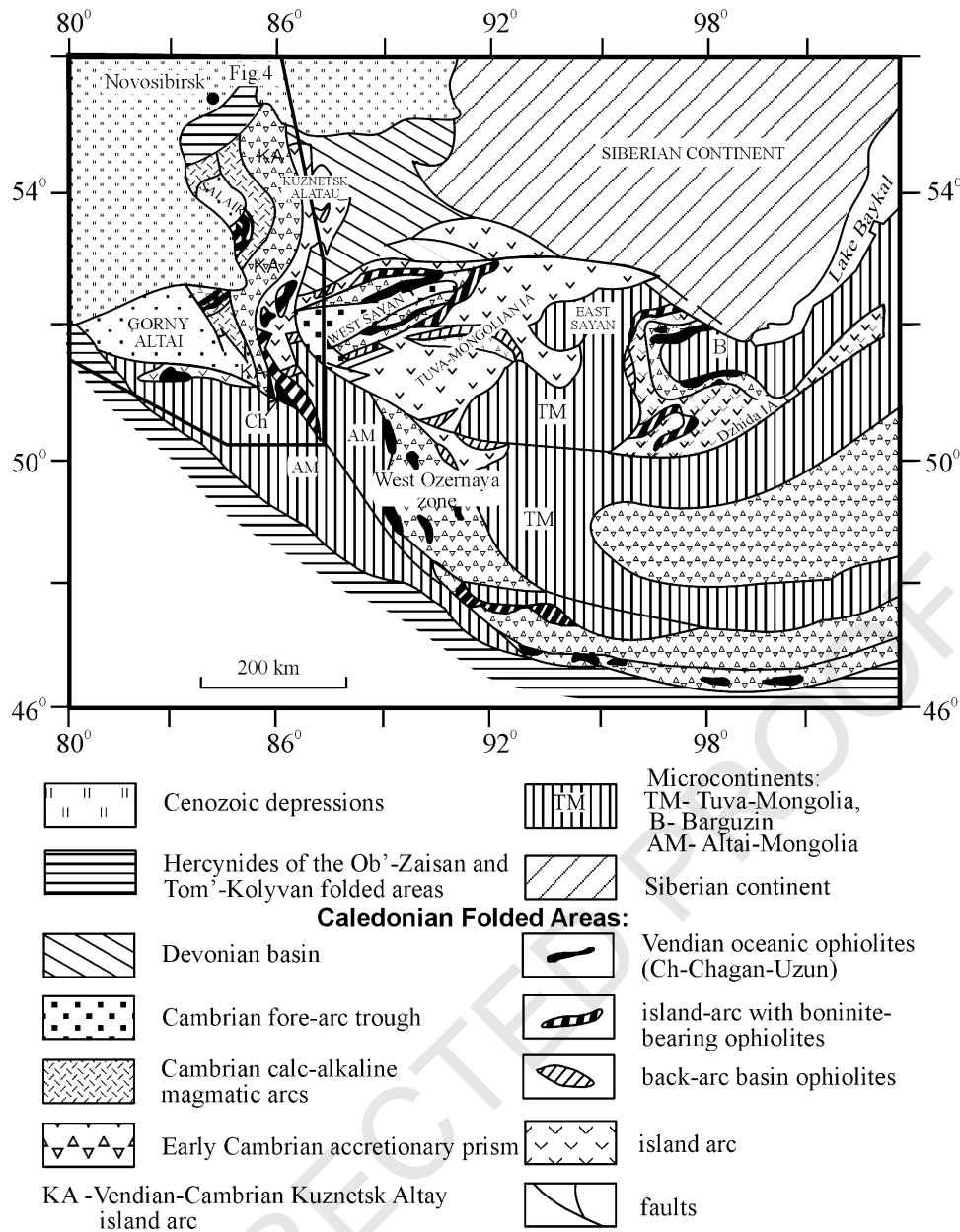


Fig. 3. The Vendian–Cambrian island arc fragments in the framework of the Siberian continent (Dobretsov et al., 1995).

the Paleo-Asian Ocean, including N-MORB and E-MORB lavas, (2) fragments of the Vendian–Early Cambrian primitive boninite–tholeiitic island arc, and (3) normal Cambrian island arc with a fore-arc basin. Typical examples of these three types of terranes occur in Gornyy Altai and Salair (Fig. 4).

There are three main accretion–collision stages in the evolution of the Paleo-Asian Ocean in Gornyy Altai and Salair (Buslov et al., 1993, 2002; Watanabe et al., 1994): (1) Early-Middle Cambrian, (2) Late Cambrian–Early Ordovician, and (3) late Paleozoic. The first and second stages characterize the evolution of the Kuznetsk–Altai and Salair island-arc systems shown in Figs. 3 and 4. In the Late Cambrian–Early Ordovician, these island-arc

systems accreted to the Siberian continent resulting in folding and thrusting and a subsequent Early Ordovician hiatus in the stratigraphic records of the studied area. The third stage includes two collisional events during the closure of the Paleo-Asian Ocean: The first event corresponds to the collision of the Gondwana–derived Altai–Mongolian terrane with the Siberian continent and the second one was caused by the collision of the Siberian continent together with the Altai–Mongolian terrane with the Kazakhstan continent (Buslov et al., 2001). In the late Paleozoic, the accretion–collision structure of the Siberian continent was disrupted by large-scale NE-striking strike-slip faults which created a typical mosaic-blocky structure and obscured the original relationships between tectonic

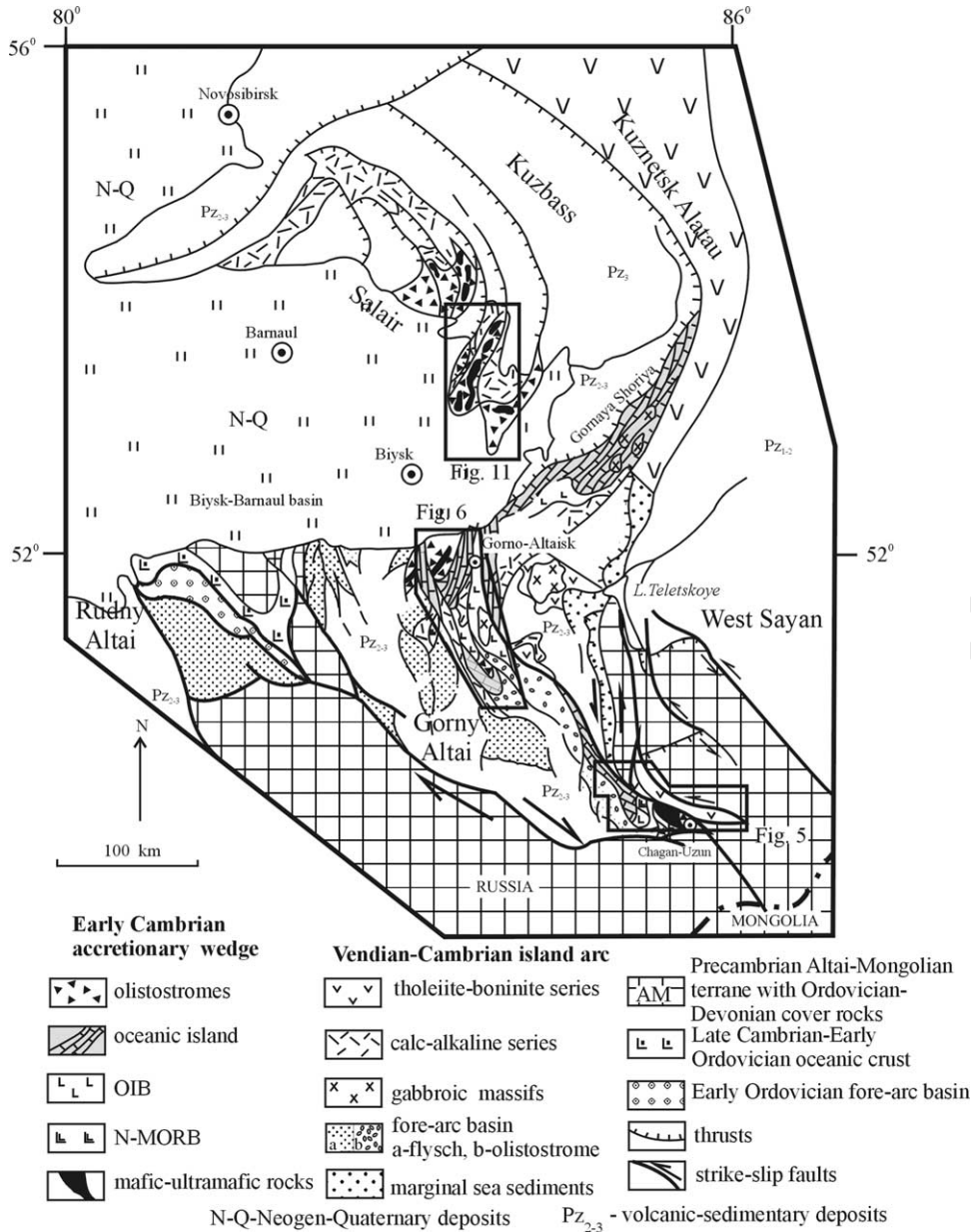


Fig. 4. Vendian–Cambrian island–arc and paleoseamant units in Gorny Altai and Salair.

units. Our study of Gorny Altai and Salair has shown that original relationships are better preserved in the western part of the Altai-Sayan area (Fig. 4).

The oceanic island units consist of pillow-lavas and their related chert-limestone sedimentary rocks. The largest paleo-islands of Katun and Baratal have been found in Gorny Altai (Figs. 5 and 6, location see in Fig. 4). The Katun terrane is more than 120 km long and up to 40 km wide. The Baratal terrane is 70 × 20 km<sup>2</sup> in size. These terranes are incorporated into the Katun and Kurai accretionary wedges, respectively. These Early–Middle Cambrian accretionary wedges also include thrust sheets of mélangé-olistostrome and ophiolites.

### 3. The Kurai accretionary wedge: structure and composition

The Kurai accretionary wedge is located in the south-eastern Gorny Altai (Figs. 4 and 5). It has been thoroughly studied in recent years. This part of Gorny Altai is well exposed and accessible. The fragments of the accretion–collision zone have been most completely preserved there (Fig. 5). Oceanic island–island arc collision was responsible for the closing of the subduction zone and exhumation of eclogites, blueschists, garnet amphibolites and metaperidotites of the Chagan-Uzun massif (Buslov et al., 1993; Buslov and Watanabe, 1996).

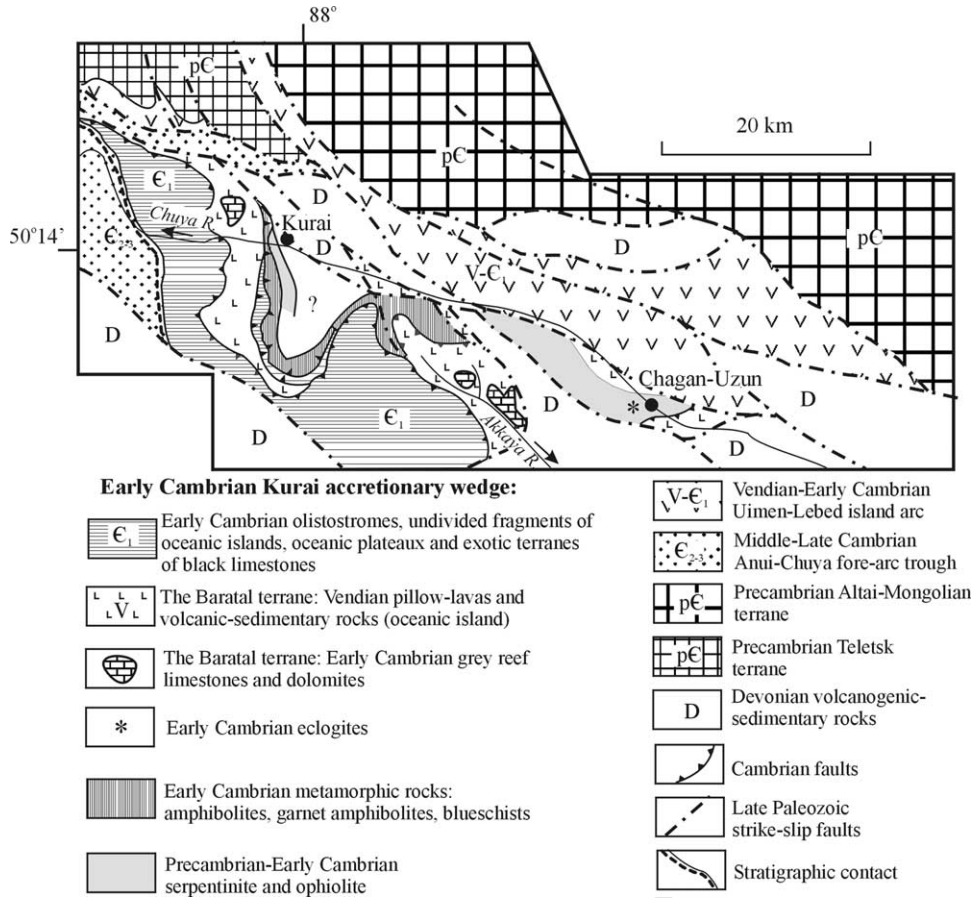


Fig. 5. The geological scheme of the Kurai accretionary wedge, showing the large fragment of the Baratal oceanic island, metamorphic and ophiolitic sheets in the basement.

The Cambrian accretionary prism (Fig. 5) hosts slivers of the Baratal oceanic island having variable composition and size. The slivers consist of oceanic sediments and oceanic island basaltic units, Chagan-Uzun oceanic ophiolites and serpentinitic mélangé with the slivers and minor blocks of eclogite, garnet amphibolite and actinolite schists. The occurrence of these metamorphic rocks is a specific feature of the Kurai accretionary prism. The barroisite–actinolite schists often occur within the accretionary prism as separate lenses. All of the above-noted slivers and blocks are associated with the Early Cambrian olistostrome. The accretionary prism was folded in the Middle–Late Paleozoic.

Sedimentary rocks of the Baratal paleo-island demonstrate changes of facies from shallow-water reef limestone, through deeper-water sedimentary-volcanogenic units, to island-slope facies represented by detrital rocks and alternation products of cherts and limestones. The slivers of paleo-island assemblages alternate with olistostrome and lenses/fragments of an exotic terrane, consisting of dark-gray to black ‘hydrosulfide’ limestones.

The dark-gray and black limestones differ from paleo-island carbonate rocks in that they are of massive texture, possess an H<sub>2</sub>S smell, and contain thin interbeds and

lenses of black cherty rocks. The black limestones contain detrital garnet, tourmaline, sillimanite, staurolite and corundum derived from metamorphic rocks of continental origin. The black limestone sequence contains no appropriate rocks for isotope dating, but Uchio et al. (2001) tried to determine the age from the black limestones using the Pb–Pb method. Their estimated age is  $577 \pm 100$  Ma.

We suggest that the dark-gray and black limestones comprised an exotic terrane which was transported into the subduction zone together with the crust of the Paleo-Asian Ocean. The thickness of tectonic sheets consisting of black limestones is 250–300 m. The limestones alternate with tectonic sheets of olistostrome. The matrix of the olistostrome consists of calcareous clay and their olistoliths are black limestones.

The Baratal paleo-island comprises three types of rocks: (1) basaltic rocks, (2) alternation of volcanic and sedimentary rocks, and (3) reef limestone. The basaltic rocks are mainly dark-gray and gray-green pillow-lavas and variolitic lavas, with subordinate amounts of amygdaloidal sub-alkaline andesitic basalts, diabase and gabbro-diabase dikes and sills. The lavas show low-temperature, greenschist facies regional metamorphism, but they still possess OIB

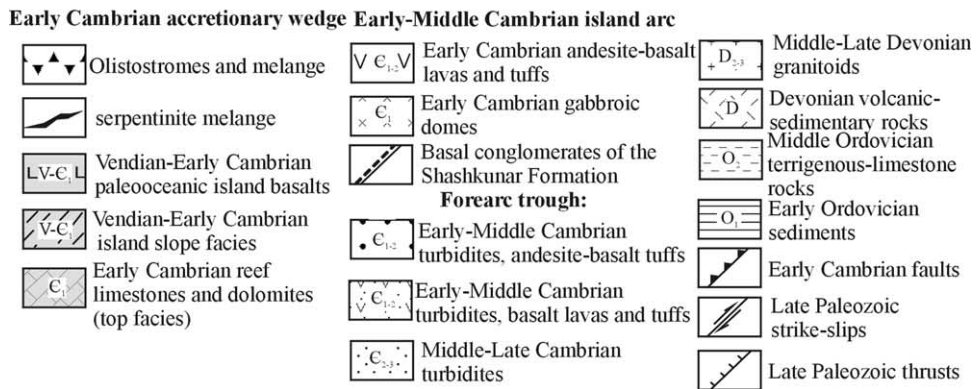
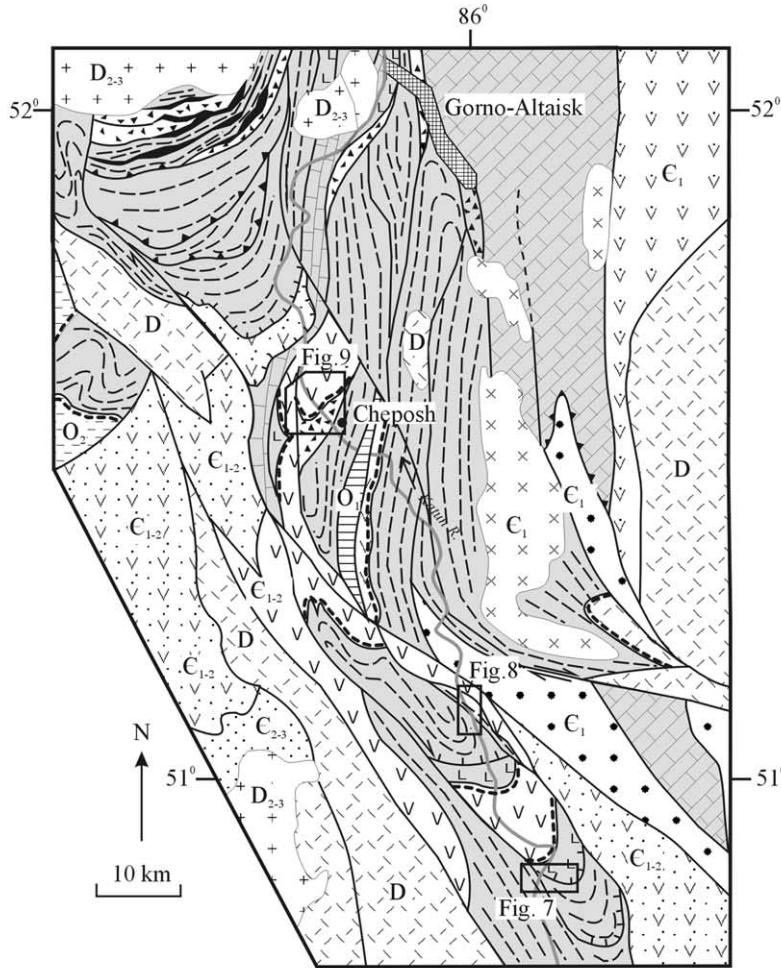


Fig. 6. The geological scheme of the Katun accretionary wedge with large fragment of the Katun paleo-oceanic island.

and MORB chemical characteristics (Gusev, 1991; Buslov et al., 1993). The magmatic rocks are associated with sparse lenses of dark-gray and gray limestone, dolomite, black and gray cherts and rarely volcanoclastic sandstone. The maximum thickness of basaltic sheets is 510 m (Gusev and Kiselev, 1988). The second rock type is mainly composed of brecciated basalts, sandstones, mudstones, tuffs, and limestone. Dark-gray or reddish layered and massive limestones intercalate with green-gray chlorite-bearing shales and tuffaceous sandstones. The presence of

numerous fine fragments of clinopyroxene, orthopyroxene, epidote, and hornblende suggests that the sedimentary rocks were deposited close to volcanoes, possibly, at the bottom of their sub-marine slopes. The fault-bounded sheets of these rocks attain a maximum thickness of 550 m (Gusev and Kiselev, 1988).

The third type of Baratal rocks includes gray reef limestones and dolomites, that once comprised the top of oceanic islands. Reef limestones and dolomites form small bodies in the Kurai zone (Fig. 5). The largest body is

785 exposed on the left bank of the river Akkaya (Fig. 5)  
 786 attaining 3 km in length and 1 km in width. These reef  
 787 limestones are underlain by conglomerates up to 4 m thick  
 788 containing fragments of basalts occurring down the  
 789 section. The thickness of the entire exposed section is  
 790 250–300 m.

791 Olistostromes that are tectonically mixed with the above  
 792 mentioned rocks are classified into: chert–limestone–  
 793 basaltic and polymictic. Gritstones and breccias comprise  
 794 the matrix of the first type olistostrome. It surrounds small  
 795 fragments of gray, light-gray and black cherts and red jasper  
 796 as well as rare basalt, carbonate, and thin-bedded carbonate  
 797 shales. The chert olistoliths are of flat or angular shape, up to  
 798 several tens of meters thick and hundreds of meters long.  
 799 The matrix of the polymictic olistostrome consists of  
 800 sandstone, clay, clay-marl and andesitic tuff. Their olisto-  
 801 liths vary in size and are represented by siliceous rocks,  
 802 limestone, dolomite, basalt and andesite.

803 Two types of olistostromes formed in different geody-  
 804 namic environments. The first type formed when an oceanic  
 805 island entered the trench. The second type formed after the  
 806 disruption of the Baratal oceanic islands terrane due to  
 807 subduction processes.

808 The Kurai accretionary wedge consists of meta-  
 809 morphic rocks and ophiolitic assemblages as it is  
 810 indicated by the section exposed to the south of Kurai  
 811 (Fig. 5). There, a volcanogenic sequence contains two  
 812 slivers of garnet amphibolite and amphibolite dipping  
 813 westward at 80°. Their thickness varies from 10 to 80 m.  
 814 The amphibolites and garnet amphibolites possess  
 815 chemical characteristics of N-MORB (Gusev, 1991;  
 816 Buslov et al., 1993). The polymictic melange includes  
 817 blocks up to several meters long of serpentinitized  
 818 pyroxene-olivine basalt, retrograde-metamorphosed garnet  
 819 amphibolites with eclogite relicts and amphibolites. Its  
 820 matrix consists of serpentinite schists and mylonites  
 821 formed after metamorphic rocks and basalts. The  
 822 serpentinitic melange consists of foliated serpentinite  
 823 incorporating blocks of massive serpentinite and light-  
 824 gray cryptocrystalline rodingite. The serpentinite bodies,  
 825 up to several meters long, extend over a distance of  
 826 many kilometers along the Baratal terrane.

827 A melange zone in the eastern part of the Kurai zone  
 828 near Chagan-Uzun Village, on the left bank of the Chuya,  
 829 consists of a 3 km-thick sequence of ultramafic rocks  
 830 which are known as the Chagan-Uzun massif. The upper  
 831 sheet of the massif is composed of massive ultramafic  
 832 rocks of weakly serpentinitized lherzolite and harzburgite  
 833 (the upper half) and massive serpentinite (the lower half).  
 834 Massive and foliated serpentinites incorporate gabbro,  
 835 gabbro-diabase and diabase dikes in the upper part, and  
 836 basalts in the lower part. The lower sheet of serpentinitic  
 837 mélange is located at the base of massive ultramafics and  
 838 contains blocks of meta-olistostrome, limestone, basalt,  
 839 silicilite, amphibolite, garnet amphibolite, and eclogite  
 840 (Buslov et al., 1993).

841 A thick serpentinite melange is present in the eastern  
 842 part, on the right bank of the Chuya River. A several  
 843 hundred meters thick metamorphic sole of garnet-free  
 844 amphibolite occurs at the contact with ultramafics and  
 845 basalts. Amphibolites of the metamorphic sole contain  
 846 relicts of a pillow-lava texture.

847 The metamorphic rocks are of special interest because  
 848 their formation and further exhumation could have been a  
 849 result of oceanic island-island arc collision during subduc-  
 850 tion. The eclogite and garnet amphibolite bodies occur in  
 851 the melange.

852 The K–Ar amphibole ages of eclogites and their  
 853 crosscutting garnet amphibolites are 535 and 487 Ma,  
 854 respectively. Buslov et al. (2002) noted Ar–Ar amphibole  
 855 ages for eclogites at about 630 Ma. The K–Ar muscovite  
 856 age of metaolistostromes is 540 Ma. The ages of 535 Ma  
 857 (amphibole in eclogite) and 540 Ma (matrix of metaolistos-  
 858 tromes) correspond to the Early Cambrian metamorphism of  
 859 subducted rocks. The K–Ar amphibole age of garnet  
 860 amphibolite is 473 Ma. The metamorphic sole at the base  
 861 of the Chagan-Uzun ophiolites consists of garnet-free  
 862 amphibolites, whose K–Ar amphibole age is 523 Ma  
 863 (Buslov and Watanabe, 1996).

864 Formally, there are three groups of geochronological  
 865 data (535–540, 523, and 473–487 Ma). They correspond to  
 866 subduction metamorphism, exhumation and later deforma-  
 867 tion processes.

868 Boudinaged and deformed gabbro, gabbro-diabase, and  
 869 diabase dikes cut the lower ophiolitic thrust sheet and are  
 870 compositionally similar to the Early–Middle Cambrian  
 871 calc-alkaline island-arc series and represent the upper age  
 872 limit of exhumation (Buslov et al., 2002). PT-estimations  
 873 for metamorphic rock assemblages of the upper thrust sheet,  
 874 including eclogites, are 13–14 kbar and 620–700 °C. They  
 875 formed at a depth of 50–60 km, whereas the metagabbro,  
 876 rodingites and garnet-free amphibolites of the lower thrust  
 877 sheet formed at 2–3 kbar (6–8 km depth). We suggest that  
 878 the upper thrust sheet with eclogites is an assemblage  
 879 of subducted rocks, whereas the garnet-free amphibolites  
 880 at the bottom of the lower thrust sheet formed later during  
 881 incorporation of hot ophiolites into the accretionary wedge  
 882 or during their thrusting over the ocean floor basalts, as was  
 883 proposed for Oman ophiolites and other similar cases  
 884 (Nicolas, 1989).

885 In general, according to the structural position, rock  
 886 assemblages, and major and trace element chemistry, the  
 887 Baratal terrane can be regarded as an oceanic island with a  
 888 fragment of oceanic crust at the base. In the earliest  
 889 Cambrian, the Baratal terrane and adjacent segments of the  
 890 oceanic lithosphere (Chagan-Uzun ophiolite) were involved  
 891 in subduction and part of its rocks underwent low- to high-  
 892 grade metamorphism. In the latest Early Cambrian, the  
 893 Baratal oceanic island closed the subduction zone and  
 894 collided with the Kurai fragment of the Uimen-Lebed  
 895 primitive island arc. This collision generated reverse  
 896 tectonic currents in the accretionary wedge and rapid



exhumation of the metamorphosed oceanic crust rocks such as the Chagan-Uzun ophiolites, eclogites and garnet amphibolites. The major and trace element chemistry of high-pressure metamorphic rocks is similar to that of MORB and OIB (Buslov et al., 1993, 2002).

#### 4. Katun accretionary wedge

The Katun accretionary wedge is situated north of the Kurai accretionary wedge and extends over a distance of more than 120 km along the Katun River, south of Gornoaltaisk (Fig. 6). It involves three types of paleo-oceanic island rock units. The Type I units consist of dark-gray bitumen-bearing limestones, black silicilites, dolomites, shales, siliceous shales, and thin basaltic flows. Sedimentary rocks dominate over volcanics. The Type II units include high-Ti tholeiites and alkaline basalts associated with lenses of cherts, carbonates and shales. The Type III units consist of reef limestone and dolomite with tuff interbeds.

These units are suggested to be fragments of a single unit of carbonate, siliceous, terrigenous and ocean island volcanic rocks formed in the oceanic island setting. Carbonate and siliceous varieties have a breccia-like texture and show traces of submarine slumping.

Fragments of paleo-oceanic islands occur in association with olistostromes of two types, e.g. siliceous–carbonate–basaltic and polymictic, analogous to the olistostromes of the Kurai accretionary wedge. The first type olistostrome formed during the ‘entrance’ of the Katun paleo-island into the trench and consists only of paleo-island fragments: basalt, chert, limestone and dolomite. The second type olistostrome consists of the same rocks plus pebbles and boulders of andesite, basaltic andesite, sandstone, mudstone and limestone which could have been transported from an island arc.

There are two types of Vendian–Early Cambrian volcanics in the Katun paleo-island: (a) thin flows of tholeiitic basalts—the relicts of oceanic crust—formed in a deep-water setting; and (b) large volcanic buildups and submarine plateaus of alkaline basalts with subordinate tholeiites. The first type of volcanic rocks are aphyric tholeiites with sporadic fine phenocrysts of olivine and clinopyroxene which possess the chemical characteristics of N-MORB (Buslov et al., 1993; Gibsher et al., 1996). The second type of volcanic rocks are olivine-bearing tholeiites, hawaiites, and alkaline basalts. The microstructure of alkaline volcanics is aphyric or Pl-porphyric (up to 10% of plagioclase phenocrysts) with an intergranular matrix containing olivine, plagioclase, and pyroxene. The olivine tholeiites are aphyric, and hawaiites (MgO = 3–5%, K<sub>2</sub>O = 0.4–0.7%) are porphyric, consisting of olivine, pyroxene and plagioclase phenocrysts and glassy matrix (Buslov et al., 1993; Gibsher et al., 1996).

The rocks of the Katun paleo-oceanic island contain abundant remnants of microphytoliths, calcareous algae and sponge spicules indicating their Late Vendian to Early Cambrian age (Terleev, 1991). Detailed description of this sequence and its list of paleontological species were reported by Terleev (1991). This paper provides a brief description of its structure, rock assemblages and microfossils.

The three sites of Edigan, Elandin and Cheposh are the best examples of the structure and rock assemblages of the Katun paleo-oceanic island. Their location is shown in Fig. 7. The Edigan site (Fig. 7) is located on the right bank of the Katun, namely in the waterdivide of its right tributaries of the Edigan and Cheba Rivers. The Edigan monocline is composed of paleo-oceanic island rocks. There are Late Vendian–Early Cambrian sedimentary rocks (Eskongin Formation), representing the slope facies of the paleo-oceanic island, and volcanics of the Manzherok Formation which consists of oceanic island bottom facies with top facies reef limestones.

The sequence of the Eskongin Formation (from Terleev (1991) with modifications) is as follows (line I–II in Fig. 7):

1. Gray and dark-gray limestones and dolomites intercalate with volcanics, tuffaceous shales and quartzites and attain a 200 m thickness.
2. Gray, dark-gray massive and fine-bedded dolomites contain clastic material and microphytoliths *Osagia tenuilamellata Reil* and attain a thickness of 140 m.
3. Intercalating terrigenous and carbonate rocks. The terrigenous sediments are shales, siliceous shales and chlorite schists, fine-clastic basaltic tuffs, and silicilith. Gray, dark-gray stratified limestone, dolomitic limestones and dolomites are present in subordinate amounts. Carbonate rocks contain remnants of sponge spicules *Monoxonellida*, *Hexactinellida*, *Tetraxonida*, and calcareous algae *Epiphyton sp.* and SSF: *Hyalithellus tenuis Cambrotubulus decurvatus*, and *Tiksitheca liscis Anabolites sp.* The thickness of the package is 300 m.
4. Gray, dark-gray massive and fine-bedded dolomites, locally with clastic material and chert interbeds (1–5 cm thick), and thin limestone and shale interbeds. Total thickness is 120 m.
5. A 60 m thick package of greenish-gray massive basaltic porphyrites.
6. Gray, dark-gray massive and fine-layered limestones contain separate thin layers of chlorite schists and cherts attaining a 160 m thickness.
7. A 400 m thick package is compositionally similar to package 3, but contains more cherts.
8. Gray, dark-gray massive and fine-bedded limestones and dolomites frequently contain terrigenous material and abundant microphytoliths (*Osagia sp.*) attaining a thickness of 100 m.

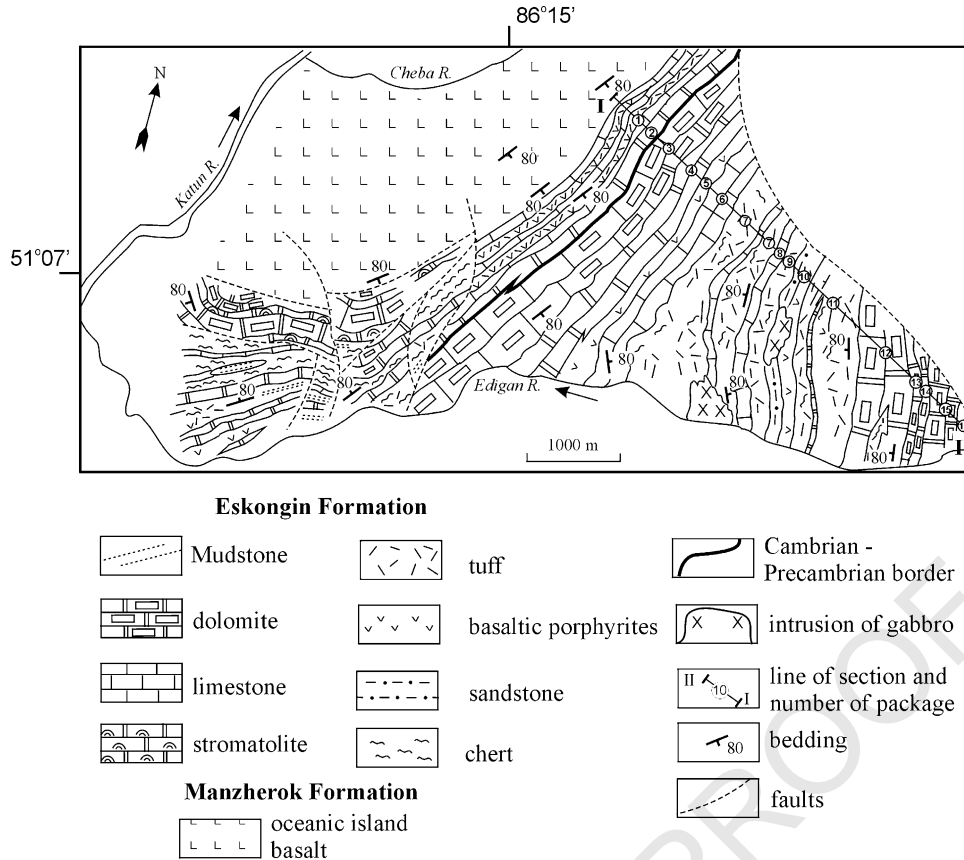


Fig. 7. The geological sketch of the Edigan site of the Katun paleo-oceanic island (from Terleev (1991) with modifications).

9. Intercalated shales and dark-gray limestones attain a 140 m thickness.
10. (A) Greenish-gray and green massive and schistose volcanics; (B) tuffaceous sandstones and siltstones with subordinate gritstones. The thickness of the package is 180 m.
11. A 400 m thick package compositionally resembles package 3.
12. Gray to dark-gray, thin-banded and massive dolomites locally contain stromatoliths and microphytoliths (*Osagia* sp., *Nubecularites catagraphus* Reilt.). Subordinate sedimentary rocks are dark limestones, black and greenish-gray tuffaceous siltstones, mudstones, and quartzites. Carbonate rocks laterally change to fine-clastic rocks. Land-slides are widespread and contain irregularly shaped bodies of carbonate rocks and siltstones. Total thickness is 450 m.
13. Intercalating dark thin-banded limestones and siltstones with chert and dolomite lenses. The thickness is 60 m.
14. Massive and stratified dark-gray/gray dolomites, limestones and tuffaceous shales 60 m thick.
15. Dark-gray to gray dolomites (up to 15 m) alternating with the above sediments involve lenses of chert and dolomite and attain a thickness of 200 m.
16. Intercalating thin beds of black limestone, black shales, green-gray tuff-siltstones attaining a total thickness of 60 m.

Sponge spicules, calcareous algae and SSF from package 3 are Lower Cambrian and the Cambrian-Precambrian boundary is at the base of this package (Terleev et al., 2003).

The total thickness of the section is 3000 m. The Eskongin Formation has a stratigraphic contact with volcanics of the Manzherok Formation. This steeply dipping contact and the presence of overturned beds suggest that siliceous sediments of the Eskongin Formation overlap the Manzherok volcanics. The basaltic sequence attains a thickness of more than 2500 m.

The *Elandin* site is located in the Katun's right bank, near its right tributary of the Chechkysh Brook (Fig. 8). Of special interest are Late Vendian–Early Cambrian reef dolomites, which we suggest were formed on top of a paleo-oceanic island. The dolomites overlap volcanic rocks of the Manzherok Formation. An interbed of sedimentary breccia consisting of volcanic boulders and pebbles is found at the base of the dolomite sequence. The light-gray to gray massive and clastic dolomites contain stromatoliths and microphytoliths and attain a thickness of 250 m. The microphytoliths are *Nubecularites punctatus* Reilt., *N.catagraphus* Reilt., *Osagia* sp., *Vesicularites flexuosus* Reilt., *Ves. lobatus* Teirl., *Ves. bothrydiophormis* (Krasn.), *Ves. reticulatus* Varizh., *Ves. igaricus* Milstein, *Ves. compositus* Z.Zhur., *Ves. pussilus* Zabr., *Nubecularites uniformis* Z.Zhur., *Ambigolamellatus horridus* Z.Zhur., *Radiusus sphaericus*

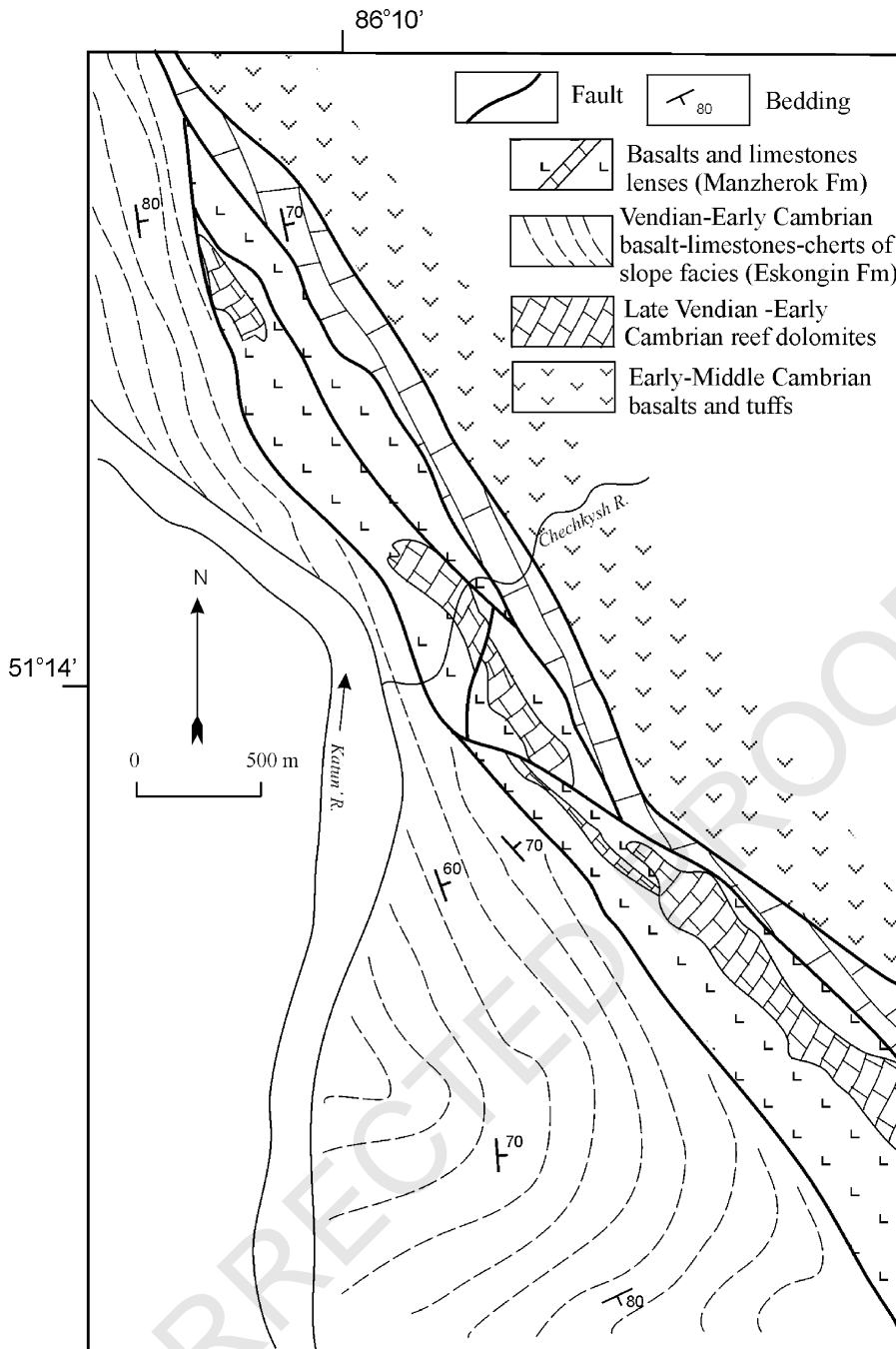


Fig. 8. The geological sketch of the Elandin site of the Katun paleo-oceanic island (from Terleev (1991) with modifications).

Z.Zhur., *Volvatella vadosa* Z.Zhur., *Glebosites gentilis* Z.Zhur., *osagia tenuilamellata* Reittl., *Vesicularites textus* Klinger, *Microphytoliths Nubecularites punctatus* and *N.catagraphus* and alga *Girvanella sp.* indicate a Late Vendian-Early Cambrian age for the dolomites (Terleev, 1991).

The Cheposh site (Fig. 9) is located in the Katun valley, near Cheposh villages (Fig. 6). There, the tectonic sheets composed of paleo-oceanic island rocks alternate with two types of deformed olistostrome. The accretionary wedge is overlapped by basal conglomerates and then

Early Cambrian (Sanashtygol Horizon)-Middle Cambrian sedimentary-volcanogenic rocks of a normal island arc (Buslov et al., 1993).

The sequence in the right bank of the Katun River (line I–II in Fig. 9) consists of several tectonic thrust sheets consisting of paleo-oceanic island rocks and olistostromes:

1. A tectonic thrust sheet composed of Type I and Type II deformed olistostromes. The Type I siliceous-carbonate-basaltic olistostrome consists of olistoliths incorporated into the breccia-sandstone matrix.

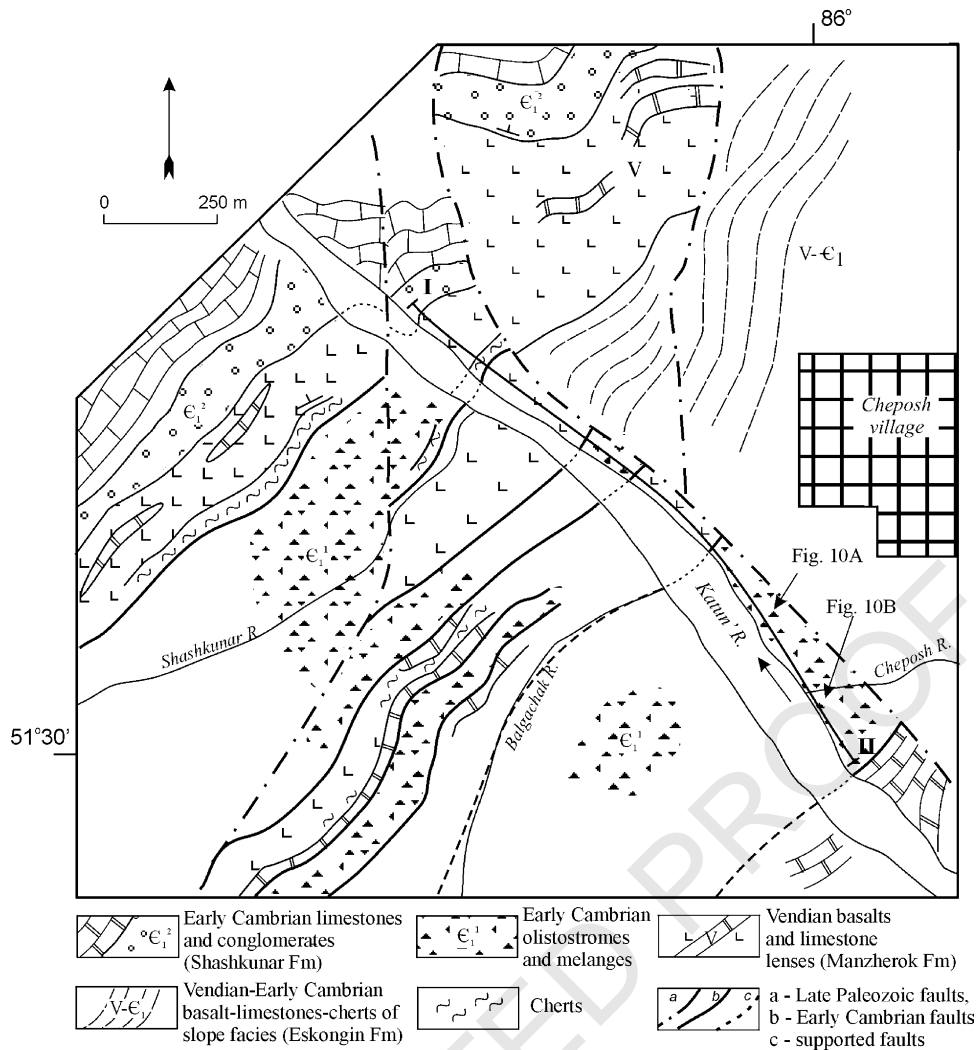


Fig. 9. The geological sketch of the Cheposh site of the Katun paleo-oceanic island (from Terleev (1991) with modifications).

Fig. 10a shows the structure of a fine-clastic olistostrome where olistoliths are several tens of centimeters in length. Large olistoliths are several hundred meters long and tens meters thick and consist of basalts and carbonate rocks. The Type II olistostrome consists of olistoliths and fine-clastic siliceous-carbonate-basaltic rocks and well-rounded boulders and pebbles of basaltic andesite, andesite, tuffs, sandstones, siltstones, and gray stratified limestones. Fig. 10b shows an outcrop in the left bank of the Cheposh mouth and the arrangement of boulders and pebbles in the sand-siltstone matrix composed of clasts of volcanic rocks, cherts, and carbonate rocks. The boulders attain 20 cm in length. The total thickness of the sheet exceeds 300 m.

2. Deformation zone composed of greenschists with blocks of basalt, chert and dolomite attains a thickness of 2–3 m.
3. A 120 m thick siliceous-carbonate-basaltic tectonic sheet.
4. Deformation zone similar to 2 of a 3–5 m thickness.
5. The 8–10 m thick Type I olistostrome.

6. Deformation zone similar to 2.
7. A 150 m thick tectonic sheet composed of pillow-lava.
8. Greenschists derived from basalts of 1–2 m thickness.
9. A 60 m thick tectonic sheet of black cherts.
10. Basaltic and carbonate rocks outcropping after a 80 m break attain a thickness of 60 m.

The Katun accretionary wedge is overlain by basal conglomerates containing carbonate rocks of the Shashkunar Formation, which occur in the lowest position of the Early–Middle Cambrian island arc sequence. The Early–Middle Cambrian age (Botomian–Amgian) of the island arc comprising the carbonate–terrigenous rocks of the Cheposh and Barangol Formations and volcanic rocks of the Ust-Syoma Formation is evidenced by numerous archaeocyathan and trilobites (Repina and Romanenko, 1964). The tectonic sheets of the accretionary wedge and carbonate rocks of the Shashkunar Formation are cross-cut by island-arc dikes of pyroxene-plagioclase porphyrites, diabase, and gabbro. The dikes preserve the original orientation and are only locally deformed. They are comagmatic with

1345  
1346  
1347  
1348  
1349  
1350  
1351  
1352  
1353  
1354  
1355  
1356  
1357  
1358  
1359  
1360  
1361  
1362  
1363  
1364  
1365  
1366  
1367  
1368  
1369  
1370  
1371  
1372  
1373  
1374  
1375  
1376  
1377  
1378  
1379  
1380  
1381  
1382  
1383  
1384  
1385  
1386  
1387  
1388  
1389  
1390  
1391  
1392  
1393  
1394  
1395  
1396  
1397  
1398  
1399  
1400

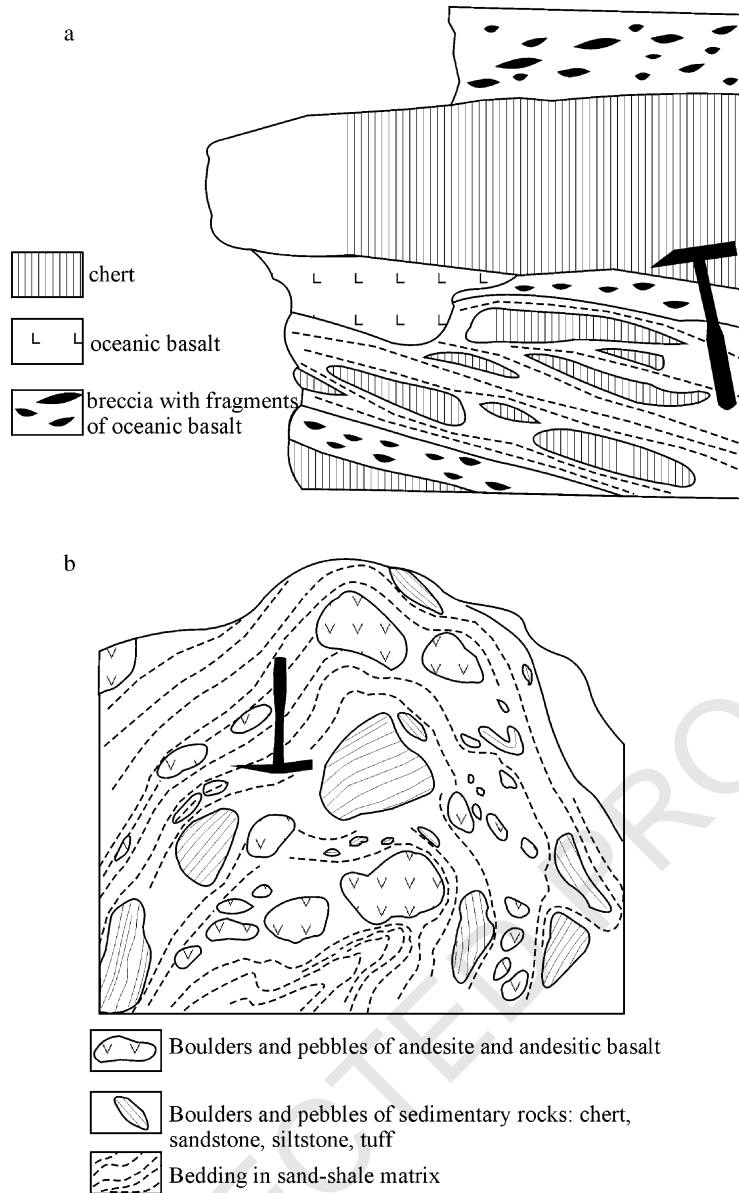


Fig. 10. The sketches of two types of tectonized olistostrome-conglomerate from the Katun River bank, near Cheposh Village (Figs. 6 and 9): a—olistostrome, b—polymyctic conglomerate.

the volcanic rocks of the Ust-Syoma Formation in the Katun zone (Fig. 6).

The Early–Middle Cambrian rocks of the normal island arc do not exhibit greenschist facies metamorphism in contrast to the accretionary wedge rocks.

Volcanogenic, siliceous-limestone and carbonate paleo-oceanic units extend to the northeast, from the Katun terrane to Gornaya Shoriya, and form a  $40 \times 250 \text{ km}^2$  structure. In the northwestern part of the Katun accretionary wedge, the tectonic sheets and olistostromes are surrounded by serpentinitic melange and basalts with N-MORB characteristics (Buslov et al., 1993; Gibsher et al., 1996). The melange consists of chrysotile-antigorite schists containing large inclusions of ultramafic rocks and gabbro. Northwards, the northwestern part of the Katun

zone is replaced by the Early Cambrian accretionary wedge of Salair.

## 5. Salair accretionary wedge

In the Salair accretionary wedge (Fig. 11), there are numerous late Paleozoic thrust and strike-slip faults. Like in the Kurai zone, there are ophiolitic rock assemblages, metamorphic rocks, and paleo-oceanic island rocks. The ophiolitic rocks are largely hidden under Meso-Cenozoic sediments of the Biya-Barnaul basin (Fig. 4). Fig. 11 shows the location of ophiolitic bodies according to borehole and geophysical data. The ophiolitic bodies are several large tectonic sheets (up to  $15 \times 5 \text{ km}^2$ ) consisting of layered

1401  
1402  
1403  
1404  
1405  
1406  
1407  
1408  
1409  
1410  
1411  
1412  
1413  
1414  
1415  
1416  
1417  
1418  
1419  
1420  
1421  
1422  
1423  
1424  
1425  
1426  
1427  
1428  
1429  
1430  
1431  
1432  
1433  
1434  
1435  
1436  
1437  
1438  
1439  
1440  
1441  
1442  
1443  
1444  
1445  
1446  
1447  
1448  
1449  
1450  
1451  
1452  
1453  
1454  
1455  
1456

1457  
1458  
1459  
1460  
1461  
1462  
1463  
1464  
1465  
1466  
1467  
1468  
1469  
1470  
1471  
1472  
1473  
1474  
1475  
1476  
1477  
1478  
1479  
1480  
1481  
1482  
1483  
1484  
1485  
1486  
1487  
1488  
1489  
1490  
1491  
1492  
1493  
1494  
1495  
1496  
1497  
1498  
1499  
1500  
1501  
1502  
1503  
1504  
1505  
1506  
1507  
1508  
1509  
1510  
1511  
1512

1513  
1514  
1515  
1516  
1517  
1518  
1519  
1520  
1521  
1522  
1523  
1524  
1525  
1526  
1527  
1528  
1529  
1530  
1531  
1532  
1533  
1534  
1535  
1536  
1537  
1538  
1539  
1540  
1541  
1542  
1543  
1544  
1545  
1546  
1547  
1548  
1549  
1550  
1551  
1552  
1553  
1554  
1555  
1556  
1557  
1558  
1559  
1560  
1561  
1562  
1563  
1564  
1565  
1566  
1567  
1568

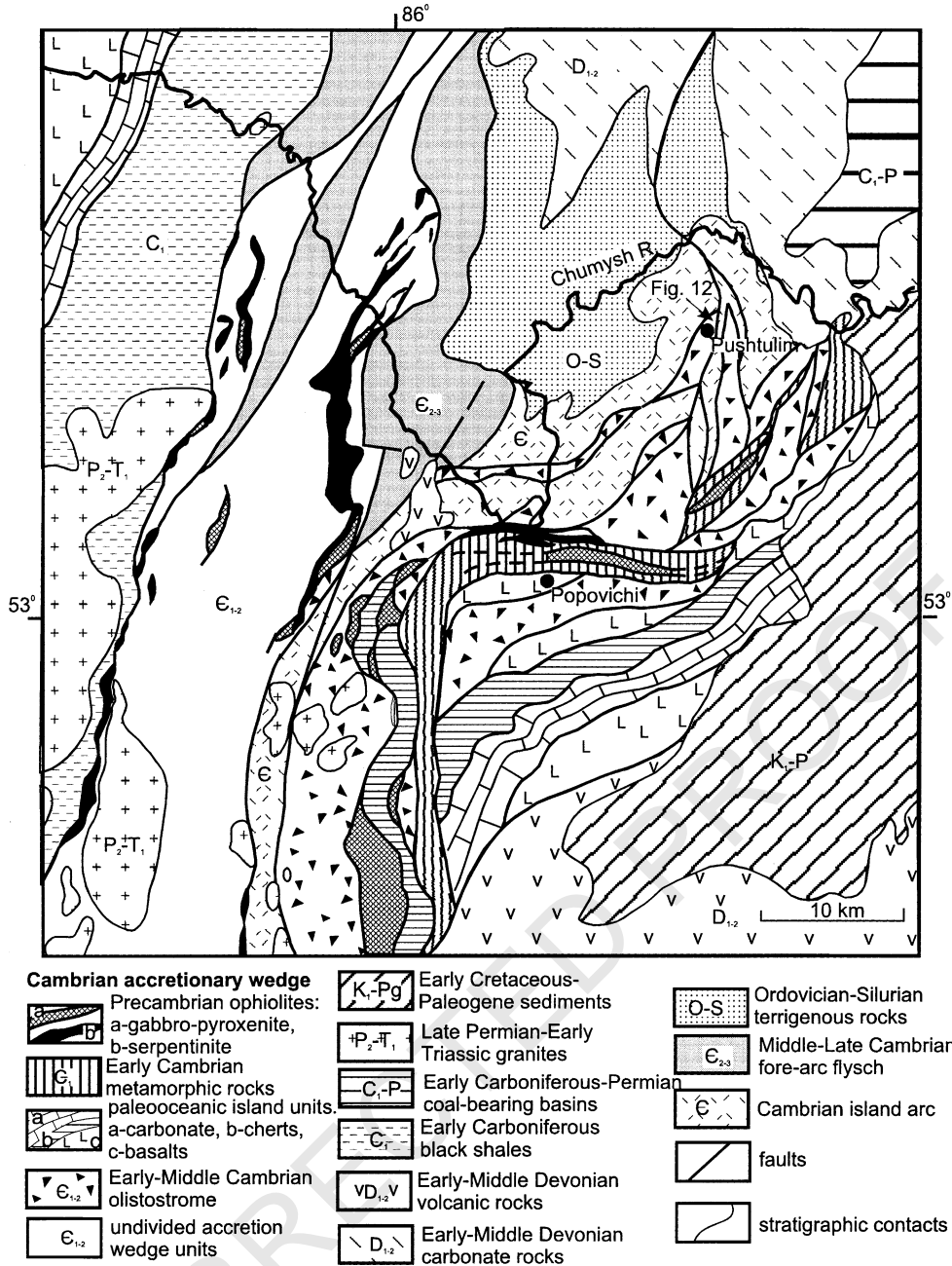


Fig. 11. The geological scheme of the Salair accretionary wedge.

pyroxenite-gabbro and serpentinitic melange. The layered gabbro-pyroxenite complex is intruded by gabbro dikes. The serpentinitic melange contains fragments of ultramafic rocks, pyroxenite, gabbro, basalt, and bedded siliceous rocks. Large carbonate-siliceous and carbonate bodies (20 × 5 km<sup>2</sup>), which were possibly fragments of an oceanic island, are associated spatially with ophiolites. The lenses of ophiolitic assemblages alternate with the olistostrome tectonic sheets. The olistostromes might occupy a large area beneath the Cenozoic sediments of the Biya-Barnaul basin.

The olistostromes are better exposed in southern Salair (Fig. 11) and contain fragments of ophiolites and oceanic islands. Olistoliths of plagioclase-bearing pillow-lavas (up to 4 × 10 m<sup>2</sup>), gabbro, clayish limestones and massive limestones occur in a rhythmically-bedded clay-sandstone groundmass, west of Popovichi Village (Fig. 11). Olistoliths of oceanic island varieties-siliceous-limestone sediments, metabasalts and tuffs-are incorporated into turbiditic matrix and are abundant in the quarry near Pushtulim Village. Fig. 12a and b show the structure of one large olistolith of sedimentary rocks. In the lower part, this olistolith consists

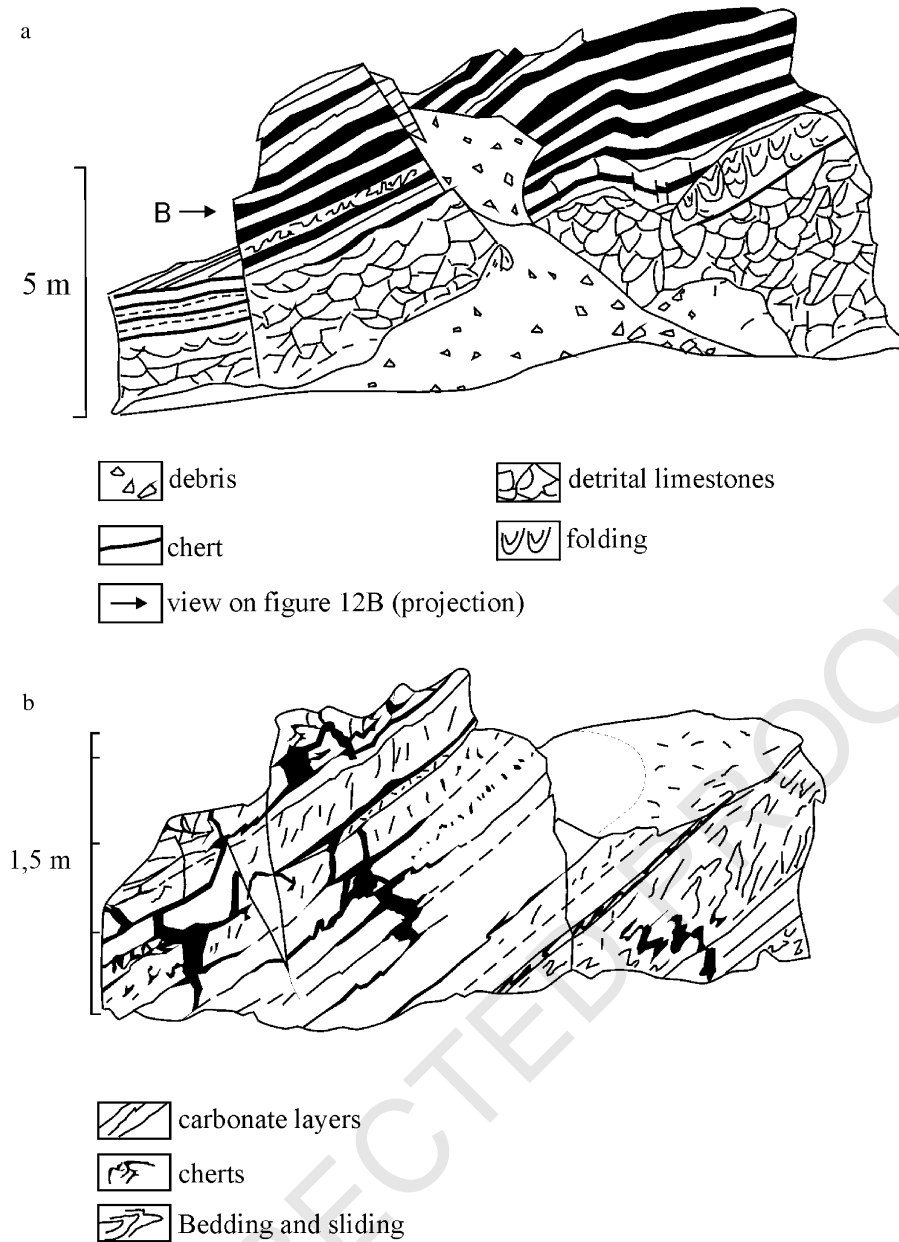


Fig. 12. Two sketches of olistostrome outcrop from the Salair accretionary wedge, near Pushtulim Village (for location see Fig. 11).

of limestone breccia and its fractures are filled with red chert. In the upper part, there are alternating limestone and siliceous beds. The limestones are seen to have undergone sliding and syndimentary folding. We suggest that the limestone-siliceous sediments originally accumulated on the oceanic island slope. Near the slope bottom, the limestones and siliceous rocks were brecciated and the fractures were filled with biosilica material (sponge spicules and radiolaria microfossils have been poorly preserved).

The metamorphic unit consists of several tectonic sheets (Fig. 11). Near Popovichi Village, there are tectonic sheets of garnet amphibolites, amphibolites, and blueschists. They are separated by tectonic lenses of graphite-bearing carbonate rocks and gabbro. These

structural units are surrounded by serpentinitic schists with fragments of pyroxenite, gabbro, diabase, basalt, and ultramafic rocks.

The oceanic island structural unit consists of several sheets of basalt, gray bedded siliceous rocks and limestones, which alternate with olistostrome lenses.

## 6. Discussion

Accretion–collisional processes obviously play a significant role in the early stages of continental crust growth. In general, the evidence for the early continental crust growth before the collision of large continents and

1681 microcontinents comes from fragments of oceanic islands  
 1682 in accretionary wedges, like in Gorny Altai and Salair,  
 1683 where we recognize three main stages of accretion–  
 1684 collisional processes. Using the Edigan site as an example,  
 1685 we can estimate the height of the paleo-oceanic islands  
 1686 (Fig. 7). Taking into account the average angle of 30° for  
 1687 the slopes of oceanic island and the 3000 m and more  
 1688 thickness of the slope deposits of the Eskongin Formation,  
 1689 the height of that volcanic buildup would be more than  
 1690 5000 m. Collision of a high paleo-oceanic island and an  
 1691 island arc resulted in several phases of accretionary wedge  
 1692 formation during the early stages of continental crust  
 1693 growth (Fig. 13):

- 1695 1. Vendian subduction of the Paleo-Asian oceanic  
 1696 crust was accompanied by formation of a primitive  
 1697 island arc.
- 1698 2. An accretionary wedge formed during the Late Vendian–  
 1699 Early Cambrian, and paleo-oceanic islands and adjacent  
 1700 oceanic lithosphere (Chagan-Uzun ophiolites) were  
 1701

- 1737 involved in subduction.
- 1738 3. The Early Cambrian collision of paleo-islands and  
 1739 accretionary wedges resulted in reverse currents and  
 1740 exhumation of subducted rocks. During the latest Early  
 1741 Cambrian, paleo-islands were incorporated in the subduc-  
 1742 tion zone and collided with the Uimen-Lebed primitive  
 1743 island arc. Due to this collision and its related reverse flows,  
 1744 the metamorphosed parts of the oceanic crust, including  
 1745 Chagan-Uzun ophiolites, eclogites, and garnet amphi-  
 1746 brites, were rapidly transported to the surface and incorpo-  
 1747 rated into the accretion wedge (Buslov et al., 1993; Buslov  
 1748 and Watanabe, 1996).
- 1749 4. In the Early–Middle Cambrian, a normal island arc was  
 1750 formed and its accretionary wedge was intruded by gabbro-  
 1751 diabase dikes.
- 1752 5. During the Middle–Late Cambrian, the Anui-Chuya fore-  
 1753 arc basin was formed.

1754  
 1755 Later, the rocks underwent Ordovician and Late  
 1756 Paleozoic folding and related deformation.  
 1757  
 1758  
 1759  
 1760  
 1761  
 1762  
 1763  
 1764  
 1765  
 1766  
 1767  
 1768  
 1769  
 1770  
 1771  
 1772  
 1773  
 1774  
 1775  
 1776  
 1777  
 1778  
 1779  
 1780  
 1781  
 1782  
 1783  
 1784  
 1785  
 1786  
 1787  
 1788  
 1789  
 1790  
 1791  
 1792

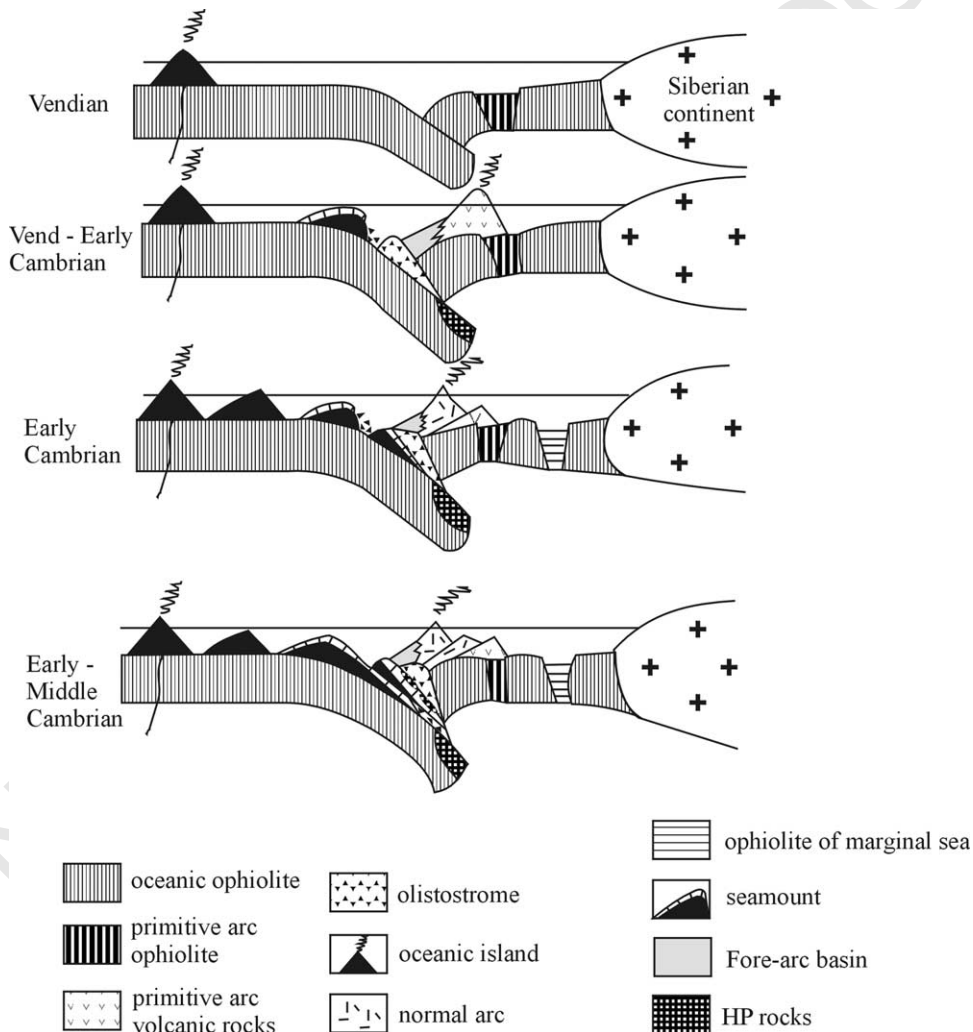


Fig. 13. Geodynamic model of the Gorny Altai and Salair accretionary wedges origin.



## 7. Conclusions

The Vendian and Early Cambrian evolution of sedimentation in the open-ocean realm is recorded in the stratigraphy of accreted oceanic rocks in the Baratal, Katun and Salair accretionary wedges. The oceanic sediments are reconstructed as extensive continuous masses ranging from a shallow-water reef complex on a basalt-based island to deep-water siliceous sediments on the ocean floor around the island. The deformation fabrics of limestone document collision of the island, in which large-scale collapse of the reef complex, probably induced by normal faulting in the outer trench-slope area, played the most important role. The collapse resulted in formation of extensive disrupted products, ‘broken’ limestone and limestone breccia. Numerous olistostrome bodies contain pebbles and boulders of island-arc rocks showing a deep-trench setting of sedimentation.

The Gorny Altai and Salair examples demonstrate that fragments of oceanic crust in the accretionary wedge consist not only of ophiolitic rock units, but also paleo-oceanic island units whose height exceeded 5000 m, and are important features in the structure of foldbelts. The study of their geochemistry, isotopic age, lithology and paleontology would allow a complete reconstruction of the ancient oceans and lead to better understanding of the petrological processes that resulted in formation of paleo-oceanic crust and early continental growth.

## 8. Uncited Reference

[Simonov et al., 1994.](#)

## Acknowledgements

This study was supported by RFBR grants no. 02-05-64627 and 03-05-64668. We are grateful for the constructive criticisms and suggestions from the reviewers. Especially we would like to express our cordial thanks for Boris Natalin for his critical reading, text edition and valuable comments. Our thanks are extended to Inna Safonova from the Institute of Geology for her help with the preparation of the English version of the manuscript and Larisa Smirnova from the same institute for her assistance with figure drawing.

## References

Ben-Avraham, Z., Nur, A., Jones, D., Cox, A., 1981. Continental accretion: from oceanic plateau to allochthonous terranes. *Science* 213, 47–54.

Berzin, N.A., Dobretsov, N.L., 1994. Geodynamic evolution of southern Siberia in Late Precambrian–Early Paleozoic time. In: Coleman, R.G.,

(Ed.), *Reconstruction of the Paleo-Asian Ocean*, VSP International Science Publishers, Utrecht, The Netherlands, pp. 53–70. 1849

Bogdanov, N.A., Dobretsov, N.L., 2002. The Okhotsk volcanic oceanic plateau. *Russian Geology and Geophysics* 43, 101–114. 1850

Buslov, M.M., Watanabe, T., 1996. Intra-subduction collision and its role in the evolution of an accretionary wedge: the Kurai zone of Gorny Altai, Central Asia. *Russian Geology and Geophysics* 36, 83–94. 1852

Buslov, M.M., Berzin, N.A., Dobretsov, N.L., Simonov, V.A., 1993. *Geology and Tectonics of Gorny Altai*. Guide-book of excursion, IGCP Project 283, United Institute of Geology, Geophysics and Mineralogy Publ, Novosibirsk. 1855

Buslov, M.M., Saphonova, I.Yu., Watanabe, T., Obut, O., Fujiwara, Y., Iwata, K., Semakov, N.N., Sugai, Y., Smirnova, L.V., Kazansky, A.Yu., 2001. Evolution of the Paleo-Asian ocean (Altai-Sayan region, Central Asia) and collision of possible Gondwana-derived terranes with the southern marginal part of the Siberian continent. *Geosciences Journal* 5, 203–224. 1856

Buslov, M.M., Watanabe, T., Saphonova, I.Yu., Iwata, K., Travin, A.V., 2002. A Vendian–Cambrian island arc system of the Siberian continent in Gorny Altai (Russia, Central Asia). *Gondwana Research* 5, 781–800. 1857

Chekhovich, V.D., 1997. On the accretion of oceanic rises. *Geotectonics* 4, 69–79. in Russian. 1858

Cloos, M., 1993. Lithospheric buoyancy and collisional orogenesis: subduction of oceanic plateaus, continental margins, island arcs, spreading ridges and islands. *Geological Society of America Bulletin* 105 (6), 715–737. 1859

Coleman, R.G., 1977. *Ophiolites*, Springer, Berlin. 1860

Collot, J.-Y., Fisher, M.A., 1991. The collision zone between the d’Entrecasteaux Ridge and New Hebrides island arc. *Journal Geophysical Research* 96, 4457–4478. 1861

Dobretsov, N.L., Zonenshain, L.P. (Eds.), 1985. *Riphean-Paleozoic Ophiolites of North Eurasia*, Nauka, Novosibirsk, in Russian. 1862

Dobretsov, N.L., Kiriyashkin, A.G., 1992. Subduction zone dynamics: models of accretionary wedge. *Ophiolite* 18 (1), 61–81. 1863

Dobretsov, N.L., Kiriyashkin, A.G., 1998. *Deep-level Geodynamics*, A.A. Balkema, Brookfield. 1864

Dobretsov, N.L., Moldovantsev, Yu.E., Kazak, A.P., 1977. *Petrology and Metamorphism of Ancient Ophiolites*, Nauka, Novosibirsk, in Russian. 1865

Dobretsov, N.L., Berzin, N.A., Buslov, M.M., 1995. Opening and tectonic evolution of the Paleo-Asian Ocean. *International Geology Review* 35, 335–360. 1866

Gibsher, A.S., Esin, S.V., Izokh, A.E., Kireev, A.D., Petrova, T.V., 1996. Cambrian diopside-bearing basalts from the Cheposh zone in Gorny Altai. *Russian Geology and Geophysics* 38, 1760–1773. 1867

Gusev, N.I., 1991. Reconstruction of geodynamic regimes for Precambrian and Cambrian volcanism in southeastern Gorny Altai. In: Kuznetsov, P.P., et al. (Eds.), *Paleogeodynamics and Formation of Mineral-rich Zones in Southern Siberia*, pp. 32–54, in Russian. 1868

Gusev, N.I., Kiselev, E.A., 1988. A Precambrian stratigraphic sequence in southeastern Gorny Altai. In: Khomentovskiy, (Ed.), *Late Precambrian and Early Paleozoic deposits in Siberia, Riphean and Vendian*, Institute of Geology and Geophysics Publ, Novosibirsk, pp. 125–134, in Russian. 1869

Kanmera, K., Sano, H., 1991. Collisional collapse and accretion of Late Paleozoic Akiyoshi island. *Episodes* 14, 217–223. 1870

Masson, D.G., Parson, L.M., Milson, J., 1990. Subduction of island at the Java trench: a view with long-range sidescan sonar. *Tectonophysics* 185, 51–65. 1871

Nicolas, A., 1989. *Structure of Ophiolites and Dynamics of Oceanic Lithosphere*, Kluwer, The Netherlands. 1872

Nur, A., Ben-Avraham, A., 1982. Oceanic plateaus, the fragmentation of continents and mountain building. *Journal of Geophysical Research* 87, 3644–3662. 1873

Repina, L.N., Romanenko, E.V., 1964. *Trilobites and Lower Cambrian Stratigraphy of Altai-Sayan folded Area*, Nauka, Moscow, in Russian. 1874

Sengor, A.M.C., Natalin, B.A., Burtman, V.S., 1993. Evolution of the Altai tectonic collage and Paleozoic crustal growth in Eurasia. *Nature* 364, 299–307. 1875

- 1905 Simonov, V.A., Dobretsov, N.L., Buslov, M.M., 1994. Boninite series in  
1906 structures of the Paleo-Asian Ocean. *Russian Geology and Geophysics*  
1907 35, 182–199. 1961
- 1908 Terleev, A.A., 1991. Stratigraphy of Vendian–Cambrian sediments of the  
1909 Katun anticline (Gorny Altai). In: Khomentovskiy, V.V., (Ed.), *Late*  
1910 *Precambrian and Early Paleozoic of Siberia*, UIGGM Publ, Novosi-  
1911 birsk, pp. 82–106, in Russian. 1962
- 1912 Terleev, A.A., Luginina, V.A., Sosnovskaya, O.V., Bagment, G.N., 2003.  
1913 Calcareous algae and the lowest Cambrian border in western Altai-  
1914 Sayan. *Russian Geology and Geophysics* in press. 1963
- 1915 Uchio, Yu., Isozaki, Yu., Nohda, S., Kawahata, H., Ota, T., Buslov, M.M.,  
1916 Maruyama, Sh., 2001. The Vendian to Cambrian Paleo-environment in  
1917 shallow mid-ocean: stratigraphy of Vendo-Cambrian seamount-top  
1918 limestone in the Gorny Altai Mountains, Southern Russia. *Gondwana*  
1919 *Research* 4, 47–48. 1964
- 1920 Von Huene, R., Scholl, D.W., 1991. Observation at convergent margins  
1921 concerning sediment subduction, subduction erosion and the growth of  
1922 continental crust. *Reviews of Geophysics* 29, 279–316. 1965
- 1923 Watanabe, T., Buslov, M.M., Koitabashi, S., 1994. Comparison of arc-  
1924 trench systems in the Early Paleozoic Gorny Altai and the Mezozoic–  
1925 Cenozoic of Japan. In: Coleman, R.G., (Ed.), *Reconstructions of the*  
1926 *Paleo-Asian Ocean*, VSP International Sciences Publishers, The  
1927 Netherlands, pp. 160–177. 1966
- 1928 Zonenshain, L.P., Kuzmin, M.I., Natapov, L.M., 1990. *Geology of the*  
1929 *USSR: A Plate Tectonic Synthesis*, Geodynamic Monograph Series,  
1930 American Geophysical Union, Washington. 1967
- 1931 1970
- 1932 1971
- 1933 1972
- 1934 1973
- 1935 1974
- 1936 1975
- 1937 1976
- 1938 1977
- 1939 1978
- 1940 1979
- 1941 1980
- 1942 1981
- 1943 1982
- 1944 1983
- 1945 1984
- 1946 1985
- 1947 1986
- 1948 1987
- 1949 1988
- 1950 1989
- 1951 1990
- 1952 1991
- 1953 1992
- 1954 1993
- 1955 1994
- 1956 1995
- 1957 1996
- 1958 1997
- 1959 1998
- 1960 1999
- 2000
- 2001
- 2002
- 2003
- 2004
- 2005
- 2006
- 2007
- 2008
- 2009
- 2010
- 2011
- 2012
- 2013
- 2014
- 2015
- 2016